Zero-energy wave packets that follow classical orbits

Adam J. Makowski* and Piotr Pepłowski†
Institute of Physics, Nicolaus Copernicus University, ul. Grudziądzka 5, 87-100 Toruń, Poland
(Received 7 August 2012; published 18 October 2012)

Coherent states for a large class of the Lenz-Demkov-Ostrovsky (LDO) potentials are constructed as superpositions of zero-energy Hamiltonian eigenstates. They represent very well-localized stationary wave packets. Moreover, it is shown how to make the packets move along suitable classical orbits. The calculations are performed for a few members of the LDO family of potentials, among them, for the Maxwell's fish-eye model and that used for a theoretical explanation of the periodic system of elements.

DOI: 10.1103/PhysRevA.86.042117 PACS number(s): 03.65.Ge, 42.50.Dv, 42.50.Ar

I. INTRODUCTION

Since the beginnings of quantum mechanics, there has been a great deal of interest in the construction and time evolution of wave packets. The contemporary development of the laser technique enables us to produce and observe well-localized packets and study various relations between classical and quantum mechanics. The wave packets were first observed some 25 years ago [1,2] and were created by photoexcitation using ultrashort pulses. A very convenient tool to produce the packets was proposed by Jones *et al.* [3] and consists in using unipolar electric-field pulses of the terahertz spectrum (half-cycle pulses). Since then, many papers have been devoted to both theoretical as well as experimental studies of packet dynamics. Some representative experimental papers on Rydberg wave packets in atoms can be found in [4,5] and those for molecules in [6].

Formally, wave packets can be derived in many ways. The most popular and best known are those based on either the construction of the coherent states as eigenstates of the lowering operator [7], creating them from the ground state with the help of a displacement operator [8], or finding minimum-uncertainty wave packets [9]. Examples of interesting theoretical studies on the subject are presented in [10,11] and a review of theoretical methods is presented in [12,13]. Also very intensively studied are nonspreading states called Trojan packets [14,15].

Our construction of spatially well-localized and nonspreading packets is not related to the above methods, but constitutes a generalization of the approach [16] used for a two-dimensional (2D) harmonic oscillator. In the present paper, the packets are superpositions of states with well-defined angular momentum and, contrary to Ref. [16], all correspond to the total energy $E = 0$. In what follows, calculations are performed for potentials in the form

$$V_k(r) = \frac{-w\rho^{2k}}{2R^2\rho^2(1+\rho^{2k})^2} = \frac{-w}{2R^2\rho^2(\rho^{-k}+\rho^k)^2}, \quad \rho \equiv \frac{r}{R}, \tag{1}$$

introduced by Lenz [17], and Demkov and Ostrovsky [18,19] (LDO).

The normalizable bound-state solutions for $E = 0$ have found many applications. For $k = 1/2$, they were used [19–21] for describing the *Aufbau* law for building up the periodic system of elements and, in [22,23], for explaining some properties of the Wannier-Mott excitons. The solutions for $k = 1$ correspond to the fish-eye model (see Ref. [24] and references therein) introduced by Maxwell a long time ago [25], and are also used [26] in the theory of quantum dots with smooth boundaries. The case of $k = 3$ has found an application [27] in explaining some grouping of levels observed in medium-size sodium clusters.

The aim of our paper is to derive wave packets for the potential in Eq. (1) for an arbitrary value of $k > 0$ and the total energy $E = 0$. Additionally, we require that the packets follow precisely classical trajectories. To this end, we first survey zero-energy solutions for the LDO potentials. Details are given in Sec. II. Then, in Sec. III, we shall derive a general formula for stationary wave packets. In Sec. IV, we show how to set in motion the constructed packets, and their time evolution is presented in a number of figures. Section V contains conclusions.

II. ZERO-ENERGY WAVE FUNCTIONS

For the class of central potentials in Eq. (1), the radial part of the two-dimensional (2D) Schrödinger equation, with the total energy $E = 0$, reads

$$\frac{d^2F}{d\rho^2} + \frac{1}{\rho}\frac{dF}{d\rho} + \left[\frac{mw}{\hbar^2}\frac{\rho^{2k}}{\rho^2(1+\rho^{2k})^2} - \frac{l^2}{\rho^2}\right]F(\rho) = 0, \tag{2}$$

where m stands for the mass of particle, l stands for angular momentum quantum numbers, $\rho = \sqrt{X^2+Y^2}$, and the coupling constant w is restricted to $w > 0$. Equation (2) has regular solutions vanishing at infinity provided that the value of w is quantized according to the rule

$$\frac{mw}{\hbar^2} = 4k^2Q(Q+1), \tag{3}$$

$$Q = n + l/k, \quad k > 0, \tag{4}$$

with $n = 0,1,2,\ldots$ denoting the radial quantum number. The solutions of Eq. (2) have the following form:

$$F_{nl}^{(k)}(\xi) = N_{nl}^{(k)}(1-\xi^2)^{l/2k}C_n^{l/k+1/2}(\xi), \tag{5}$$

*amak@fizyka.umk.pl
†peplow@fizyka.umk.pl

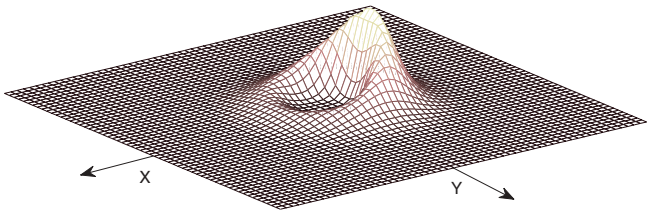

FIG. 1. (Color online) The probability density $|\Psi^{(k)}_{\alpha\beta}(X,Y)|^2$ for the zero-energy coherent state, given by Eq. (12), with $\alpha = 0.75$, $\beta = 1$, and $k = 2$. Its contour plot is given in Fig. 4(a). The coordinates X and Y are dimensionless.

where

$$\xi = \frac{1-\rho^{2k}}{1+\rho^{2k}} \tag{6}$$

and $C^{\gamma}_n(\xi)$ are the Gegenbauer polynomials. Thus, the full solution, including the angle factor, has the form

$$\Phi^{(k)}_{nl}(\xi,\varphi) = N_\varphi \exp(il\varphi) F^{(k)}_{nl}(\xi). \tag{7}$$

The square-integrable solutions for the LDO potentials in Eq. (1) were first found in 3D configural space in [18,19], whereas they were found in 2D space in [20], and those generalized to arbitrary dimensions were found in [28].

In spite of its tedious calculations, the normalization of radial wave functions, including the 2D case

$$\int_0^\infty \left[F^{(k)}_{nl}(\rho)\right]^2 \rho d\rho = 1, \tag{8}$$

can be formally done as described in [28], where an example is worked out for $k = 1$. In any case, no simple expression can be derived for the constants $N^{(k)}_{nl}$. However, we do not need any explicit formula for them. It is only important that the functions in Eq. (5) obey the condition (8) for $l > 1$.

III. STATIONARY WAVE PACKETS

We shall now construct a spatially well-localized state composed of the following combination of states (7):

$$\Psi^{(k)}_{\alpha\beta}(\xi,\varphi) = N(\alpha,\beta) \sum_{l=2}^{\infty}\sum_{n=0}^{\infty} \left[N_\varphi N^{(k)}_{nl}\right]^{-1} \frac{\alpha^n \beta^l}{l!} \Phi^{(k)}_{nl}(\xi,\varphi). \tag{9}$$

The parameters α and β, complex in general, can be taken real without loss of generality. The symbols $N(\alpha,\beta)$, N_φ, and $N^{(k)}_{nl}$ stand for the normalization of corresponding states. Though the sums constitute a superposition of states associated with different coupling constants w [Eqs. (3) and (4)], the corresponding potential in Eq. (1) is still invariant in shape. Whatever is the value of w, and hence of the quantum numbers $n \geqslant 0$ and $l \geqslant 2$, the sums combine states, *all* corresponding to the same energy $E = 0$. In this case, with growing w, the kinetic energy of the particle is growing as well, and the ratio of the kinetic and potential energies is a constant. This is a consequence of conservation of the total energy $E = 0$.

Now, using Eqs. (7) and (5), and the formula [29]

$$\sum_{n=0}^{\infty} a^n C^{l/k+1/2}_n(\xi) = (1-2a\xi+a^2)^{-l/k-1/2}, \quad |\alpha| < 1, \tag{10}$$

we get

$$\Psi^{(k)}_{\alpha\beta}(\xi,\varphi) = \frac{N(\alpha,\beta)}{\sqrt{1-2\alpha\xi+\alpha^2}} \sum_{l=2}^{\infty} \frac{1}{l!} \left[\frac{\beta \exp(i\varphi)(1-\xi^2)^{1/(2k)}}{(1-2\alpha\xi+\alpha^2)^{1/k}}\right]^l. \tag{11}$$

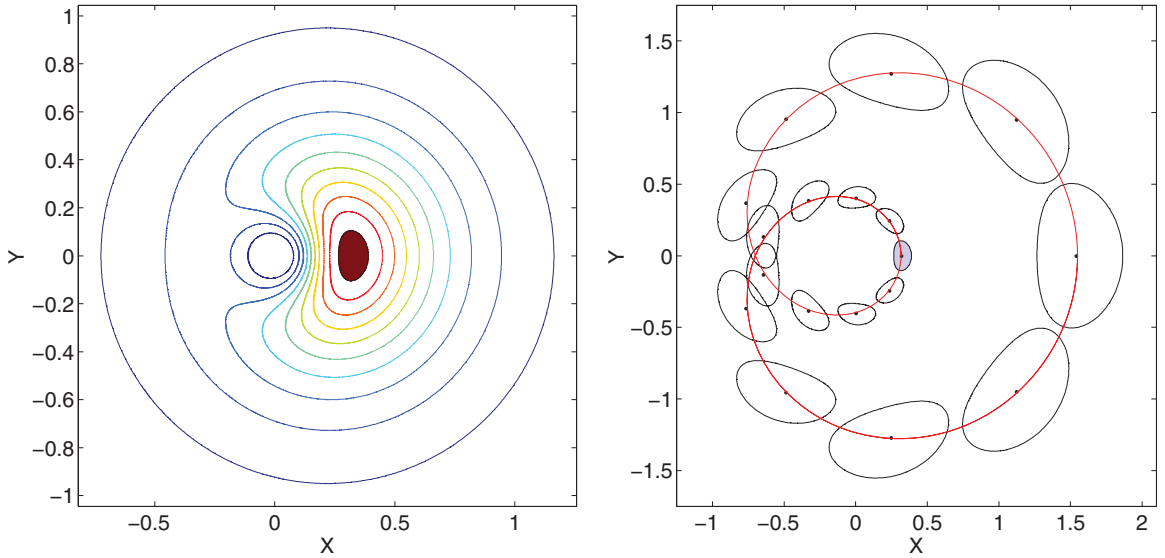

FIG. 2. (Color online) (a) Contour lines of the probability density $|\Psi^{(k)}_{\alpha\beta}(X,Y)|^2$ for $k = 1/2$, $\alpha = 0.21$, and $\beta = 1$. The shaded contour is for $|\Psi^{(k)}_{\alpha\beta}(X,Y)|^2 = 0.95$. (b) The time evolution of the stationary packet, given by Eq. (12), according to Eq. (18). The contour of constant density is plotted for equidistant instants of time. Its initial position for $\tau = 0$ is marked by the shaded area. The figure is for $k = 1/2, \alpha = 0.21$, and $\beta = 1$. Dots represent the positions of the packet's maxima and the continuous line depicts the corresponding classical orbit from Eq. (22), where $C_2 = 0$, $C_1 = 0.475$, and $\varphi_0 = \pi$. The coordinates X and Y are dimensionless.

Obviously, the sum over l can be performed as well, and finally, for the probability density, we obtain

$$\left|\Psi_{\alpha\beta}^{(k)}(X,Y)\right|^2 = \frac{N^2(\alpha,\beta)}{1-2\alpha\xi+\alpha^2}\{1+A^2+2A\cos(\varphi) + \exp[2A\cos(\varphi)] - 2\exp[A\cos(\varphi)] \times (\cos[A\sin(\varphi)] + A\cos[A\sin(\varphi)-\varphi])\}, \tag{12}$$

where

$$A = \frac{\beta(1-\xi^2)^{(1/(2k))}}{(1-2\alpha\xi+\alpha^2)^{1/k}}, \tag{13}$$

$\varphi = \tan^{-1}(Y/X)$, and ξ is defined in Eq. (6).

Note that the sum over l in Eq. (11) starts from the value of $l = 2$, which is a crucial point in our calculations. If the values of $l = 0$ and $l = 1$ were allowed as well, we would get in Eq. (12) merely the fourth term in the curl brackets. In such a case, the resulting probability density does not vanish at infinity. For our packet, when $\xi = 1$ ($\rho = 0$) and $\xi = -1$($\rho \to \infty$), in both cases $A = 0$ and $|\Psi_{\alpha\beta}^{(k)}(X,Y)|^2$ tends to zero. Its image is given in Fig. 1 and shows that the probability density forms up into a well-localized wave packet. Numerical tests show that its general shape is about the same for all values of k (see below), i.e., for a large class of the LDO focusing potentials in Eq. (1). It is also noticeable that a contemporary pico- and femtosecond laser technique has provided tools to produce and control packets of this shape [4].

IV. PACKETS THAT FOLLOW CLASSICAL ORBITS

The question emerges of how to set the stationary packet in motion; even more, how to make it move along classical orbits. The standard method of quantum mechanics consists in using the time-shift operator, say $\hat{T}_t$, and then $\psi(t) = \hat{T}_t\psi(t=0)$. For time-independent Hamiltonians, it reads as $\hat{T}_t = \exp(-\frac{i}{\hbar}\hat{H}t)$. In our case, the states composing the wave packet (12) are all zero-energy eigenstates of the Hamiltonian. Thus, the above approach does not apply here and, instead, we propose the following way.

By defining the operator

$$G = -\frac{\rho^2(1+\rho^{2k})^2}{4k^2\rho^{2k}}\left(\frac{\partial^2}{\partial\rho^2}+\frac{1}{\rho}\frac{\partial}{\partial\rho}+\frac{1}{\rho^2}\frac{\partial^2}{\partial\varphi^2}\right), \tag{14}$$

Eq. (2) can be written in the Sturm-Liouville form

$$GF(\rho) = Q(Q+1)F(\rho). \tag{15}$$

Now, we can replace the quantum number Q by the operator $i\partial/\partial\tau$ and the wave functions $\Phi_{nl}^{(k)}(\xi,\varphi)$ in Eq. (7) by

$$f_{nl}^{(k)}(\xi,\varphi,\tau) = \exp(-iQ\tau)\Phi_{nl}^{(k)}(\xi,\varphi). \tag{16}$$

Since $i(\partial/\partial\tau)\exp(-iQ\tau) = Q\exp(-iQ\tau)$, the generalized version of Eq. (15) reads

$$\left[G - i\frac{\partial}{\partial\tau}\left(i\frac{\partial}{\partial\tau}+1\right)\right]f_{nl}^{(k)}(\xi,\varphi,\tau) = 0, \tag{17}$$

where the wave functions (16) obey also Eq. (2). An equation of this form was used in [20] for a group-theoretical analysis of dynamical symmetries of the LDO potentials for the special case of $k = 1/2$.

On the other hand, we know that scalar potentials are determined, in the simplest case, with the accuracy to an additive constant. So, for the potentials in Eq. (1), we can write $V_k \to V_k + C$. The choice of the constant C is a matter of the problem under consideration. The above scaling of our potentials results in the appearance of an additional phase factor, $\exp(-iC\tau/\hbar)$, which, with the choice of $C = \hbar Q$, leads to the functions $f_{nl}^{(k)}(\xi,\varphi,\tau)$ in Eq. (16). We claim here that replacing in Eq. (9) the functions $\Phi_{nl}^{(k)}(\xi,\varphi)$ by the new ones $f_{nl}^{(k)}(\xi,\varphi,\tau)$ leads to the τ-dependent analog of the stationary packet in Eq. (12), which now moves as a classical particle in the potential of Eq. (1). From a technical point of view, the same final result can be achieved if, in the summands of

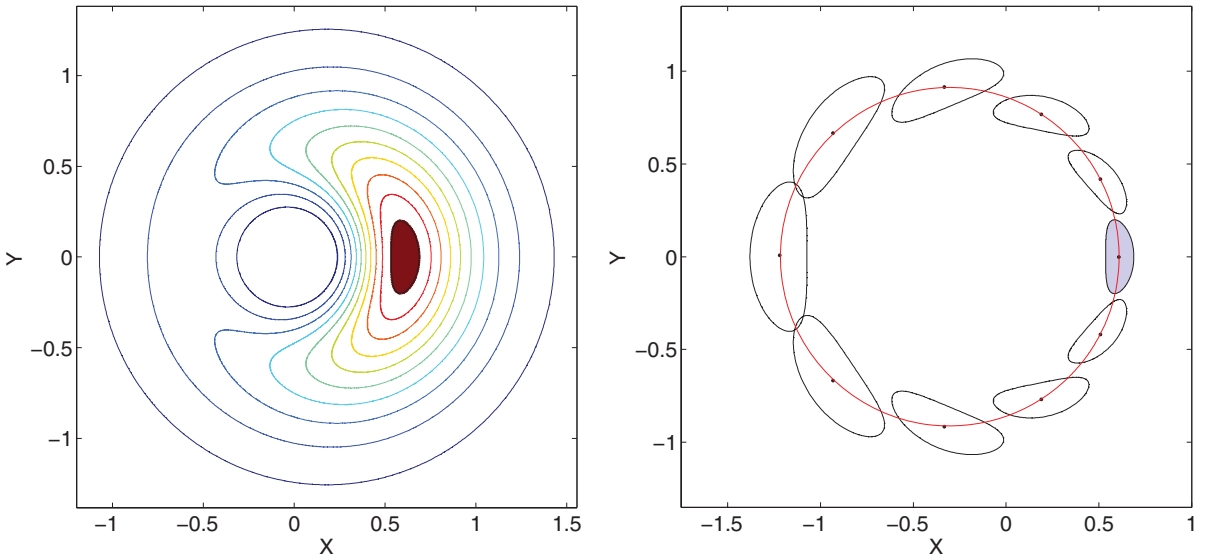

FIG. 3. (Color online) As in Fig. 2, but for $\alpha = 0.2$, $k = 1$, $C_1 = 0.353$, and $\varphi_0 = \pi/2$.

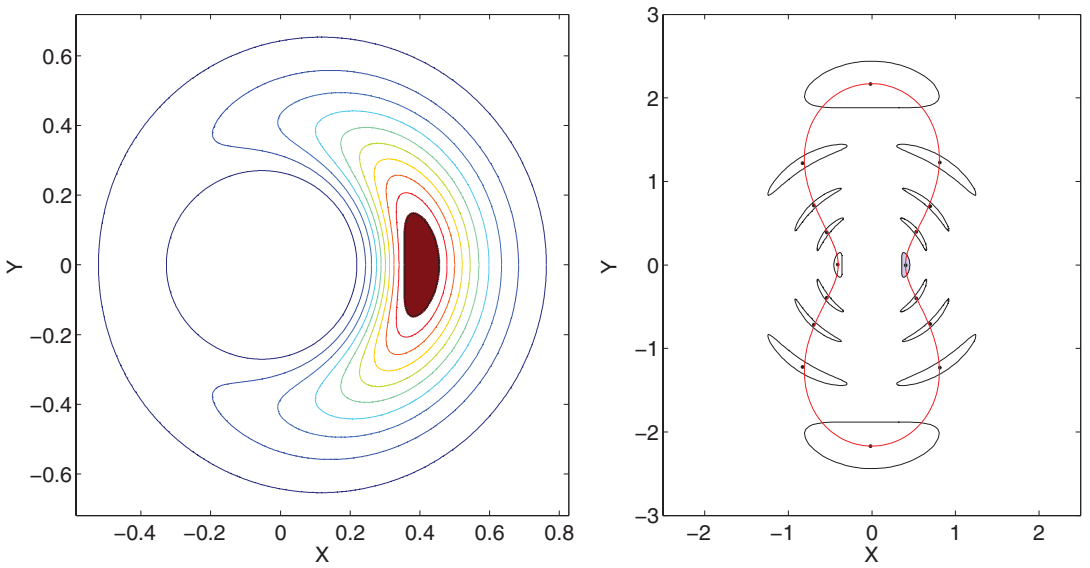

FIG. 4. (Color online) As in Fig. 2, but for $\alpha = 0.75$, $|\Psi^{(k)}_{\alpha\beta}(X,Y)|^2 = 0.9$, $k = 2$, $C_1 = 2.6$, and $\varphi_0 = \pi/4$.

Eq. (9), the parameter α is replaced by $\alpha\exp(-i\tau)$ and β by $\beta\exp(-i\tau/k)$.

The parameter τ is not a fictitious time. It is a "genuine" time, as in the Newtonian mechanics, since it orders packet positions from the earlier through the present into the future, in perfect agreement with the classical particle's actual position within the same force field. It is also a genuine time from another point of view. Only with τ introduced in this paper, the packet evolution is unitary and hence its norm is preserved. Formally, we have $i\hbar\partial\psi/\partial\tau = (\hat{T} + V_k + C)\psi(\mathbf{r},\tau)$. Then, with the substitution $\psi(\mathbf{r},\tau) = \exp[(-i/\hbar)C\tau]\phi(\mathbf{r})$, we get $(\hat{T} + V_k)\phi(\mathbf{r}) = 0$, and square-integrable solutions of this equation are used in the construction of our coherent state.

Now, making the replacements and repeating the calculations as in Sec. III, we get

$$\left|\Psi^{(k)}_{\alpha\beta}(X,Y,\tau)\right|^2 = \frac{N^2(\alpha,\beta)}{\sqrt{M}}\Big\{1 + A_\tau^2 + 2A_\tau\cos(\theta) + \exp[2A_\tau\cos(\theta)] - 2\exp[A_\tau\cos(\theta)] \times (\cos[A_\tau\sin(\theta)] + A_\tau\cos[A_\tau\sin(\theta) - \theta])\Big\}, \tag{18}$$

where

$$M = 1 + \alpha^4 + 4\alpha^2\xi^2 - 4\alpha(1+\alpha^2)\xi\cos(\tau) + 2\alpha^2\cos(2\tau), \tag{19}$$

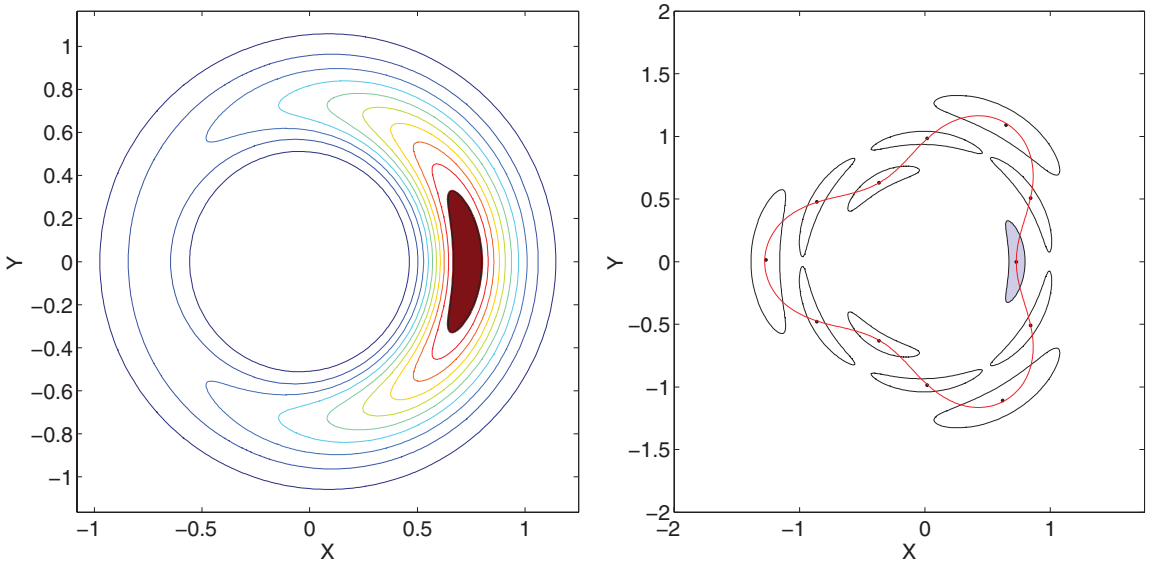

FIG. 5. (Color online) As in Fig. 2, but for $\alpha = 0.5$, $|\Psi^{(k)}_{\alpha\beta}(X,Y)|^2 = 0.9$, $k = 3$, $C_1 = 0.95$, and $\varphi_0 = \pi/6$.

$$A_\tau = \beta \left(\frac{1-\xi^2}{M} \right)^{1/(2k)}, \tag{20}$$

and

$$\theta = \frac{1}{k} \tan^{-1} \left[\frac{\sin(k\varphi - \tau) - 2\alpha\xi \sin(k\varphi) + \alpha^2 \sin(k\varphi + \tau)}{\cos(k\varphi - \tau) - 2\alpha\xi \cos(k\varphi) + \alpha^2 \cos(k\varphi + \tau)} \right]. \tag{21}$$

When $\tau = 0$, we have $\sqrt{M} = 1 - 2\alpha\xi + \alpha^2$, $A_\tau = A$, $\theta = \varphi$, and $|\Psi^{(k)}_{\alpha\beta}(X,Y,\tau)|^2 = |\Psi^{(k)}_{\alpha\beta}(X,Y)|^2$. Let us remember that $\xi = (1-\rho^{2k})/(1+\rho^{2k})$, $\rho^2 = X^2 + Y^2$, and $\varphi = \tan^{-1}(Y/X)$.

Note also that classical equations of motion can be formally integrated for $E = 0$ for all potentials in Eq. (1), and the result can be given in the form [28]

$$\rho^k - \rho^{-k} = 2\{C_1 \sin[k(\varphi - \varphi_0)] + C_2 \cos[k(\varphi - \varphi_0)]\}, \tag{22}$$

where, for the real constants of integration, we have $C_1^2 + C_2^2 = \frac{m w_c}{4 L_c^2} - 1$, and w_c and L_c stand for the classical coupling constant and angular momentum, respectively.

Accepting τ as a dimensionless time, we can observe that the packet in Eq. (18) precisely follows classical orbits of Eq. (22) for all values of k. Now, the time evolution of the packet is presented in a number of figures. Its normalization, i.e., the value of $N^2(\alpha,\beta)$, is found numerically for particular cases and, of course, is conserved during the packet's motion.

The shape of our packet is visualized in Figs. 2(a)–5(a) by contour lines of constant probability density. With growing value of k, the packet spreads out without changing its general shape as presented in Fig. 1. In Figs. 2(b)–5(b), we show the time evolution for equidistant instants of time τ. For $k = 1/2$ [Fig. 2(b)], the packet follows a limaçon of Pascal shaped curve obtained from Eq. (22), where dots point the positions of the packet's maxima and the shaded "bean" is for $\tau = 0$. The breathing of the distinguished contour is also seen. When $k = 1$ [Fig. 3(b)], the packet follows a circle; in Figs. 4(b) and 5(b), respectively, for $k = 2$ and $k = 3$, the packet follows more complex curves. In each case, the packet's trajectory is in excellent agreement with the corresponding classical solution.

V. CONCLUSION

In this paper, we have been concerned with the construction of two-dimensional wave packets for a class of physically important potentials of the Lenz-Demkov-Ostrovsky type. The construction involves in each case the zero-energy square-integrable Hamiltonian eigenstates. We have shown that their suitable combination leads to very well-localized packets. As a separate problem, we have discussed a possible way of setting the states in motion. The idea used here of gauging potentials to get the required packet trajectories seems to be a proper approach to the zero-energy wave packets. However, it is not clear at present how to do that for other potentials and we leave the problem for future studies. Anyway, the method proposed in our paper results in obtaining the observed very good quantum-classical correspondence.

[1] A. ten Wolde, L. D. Noordam, A. Lagendijk, and H. B. van Linden van den Heuvell, Phys. Rev. Lett. **61**, 2099 (1988).
[2] J. A. Yeazell, M. Mallalieu, J. Parker, and C. R. Stroud, Jr., Phys. Rev. A **40**, 5040 (1989).
[3] R. R. Jones, D. You, and P. H. Bucksbaum, Phys. Rev. Lett. **70**, 1236 (1993).
[4] Z. D. Gaeta, M. W. Noel, and C. R. Stroud, Jr., Phys. Rev. Lett. **73**, 636 (1994).
[5] Z. D. Gaeta and C. R. Stroud, Jr., Phys. Rev. A **42**, 6308 (1990).
[6] H. H. Fielding, Annu. Rev. Phys. Chem. **56**, 91 (2005).
[7] R. J. Glauber, Phys. Rev. **131**, 2766 (1963); A. O. Barut and L. Girardello, Commun. Math. Phys. **21**, 41 (1971).
[8] A. M. Perelomov, Commun. Math. Phys. **26**, 222 (1972).
[9] M. M. Nieto and L. M. Simmons, Jr., Phys. Rev. Lett. **41**, 207 (1978).
[10] M. Nauenberg, Phys. Rev. A **40**, 1133 (1989).
[11] J-C. Gay, D. Delande, and A. Bommier, Phys. Rev. A **39**, 6587 (1989).
[12] V. V. Dodonov, J. Opt. B: Quantum Semiclass. Opt. **4**, R1 (2002).
[13] A. Buchleiter, D. Delande, and J. Zakrzewski, Phys. Rep. **368**, 409 (2002).
[14] M. Kaliński and J. H. Eberly, Phys. Rev. A **53**, 1715 (1996).
[15] I. Białynicki-Birula, M. Kaliński, and J. H. Eberly, Phys. Rev. Lett. **73**, 1777 (1994).
[16] E. Colavita and S. Hacyan, Phys. Lett. A **337**, 183 (2005).
[17] W. Lenz, in *Problems of Modern Physics*, edited by P. Debye (S. Hirsel, Leipzig, 1928).
[18] Yu. N. Demkov and V. N. Ostrovsky, Zh. Eksp. Teor. Fiz. **60**, 2011 (1971) [Sov. Phys. JETP **33**, 1083 (1971)].
[19] Yu. N. Demkov and V. N. Ostrovsky, Zh. Eksp. Teor. Fiz. **62**, 125 (1972); **63**, 2376 (1972) [Sov. Phys. JETP **35**, 66 (1972)].
[20] Y. Kitagawara and A. O. Barut, J. Phys. B: At. Mol. Phys. **16**, 3305 (1983).
[21] Y. Kitagawara and A. O. Barut, J. Phys. B: At. Mol. Phys. **17**, 4251 (1984).
[22] A. J. Makowski, Phys. Rev. A **83**, 022104 (2011).
[23] A. J. Makowski, Phys. Rev. A **84**, 022108 (2011).
[24] A. J. Makowski, Phys. Rev. A **81**, 052109 (2010).
[25] J. C. Maxwell, Cambridge Dublin Math. J. **8**, 188 (1854); *The Scientific Papers* (Dover, New York, 1952).
[26] S. De Fillippo, M. Salerno, and V. Z. Enolskii, Phys. Lett. A **276**, 240 (2000).
[27] V. N. Ostrovsky, Phys. Rev. A **56**, 626 (1997).
[28] A. J. Makowski and K. J. Górska, Phys. Rev. A **79**, 052116 (2009).
[29] H. Bateman and A. Erdélyi, *Tables of Integral Transforms* (McGraw-Hill, New York, 1954), Vol. II.